JOURNAL OF BACTERIOLOGY, Jan. 1998, p. 377–387 Vol. 180, No. 2
0021-9193/98/$04.00+0

Identification and Characterization of *Escherichia coli* DNA Helicase II Mutants That Exhibit Increased Unwinding Efficiency

GANG ZHANG,† ENXIN DENG, LARRY BAUGH, AND SIDNEY R. KUSHNER*

Department of Genetics, University of Georgia, Athens, Georgia 30602

Received 23 July 1997/Accepted 13 November 1997

Using a combination of both ethyl methanesulfonate and site-directed mutagenesis, we have identified a region in DNA helicase II (UvrD) from *Escherichia coli* that is required for biological function but lies outside of any of the seven conserved motifs (T. C. Hodgman, Nature 333:22–23, 1988) associated with the superfamily of proteins of which it is a member. Located between amino acids 403 and 409, alterations in the amino acid sequence DDAAFER lead to both temperature-sensitive and dominant *uvrD* mutations. The *uvrD300* (A406T) and *uvrD301* (A406V) alleles produce UV sensitivity at 44°C but do not affect sensitivity to methyl methanesulfonate (MMS). In contrast, the *uvrD303* mutation (D403AD404A) causes increased sensitivity to both UV and MMS and is dominant to $uvrD^+$ when present at six to eight copies per cell. Several of the alleles demonstrated a strong antimutator phenotype. In addition, conjugal recombination is reduced 10-fold in *uvrD303* strains. Of all of the amino acid substitutions tested, only an alanine-to-serine change at position 406 (*uvrD302*) was neutral. To determine the biochemical basis for the observed phenotypes, we overexpressed and purified the UvrD303 protein from a *uvrDΔ294* deletion background and characterized its enzymatic activities. The highly unusual UvrD303 protein exhibits a higher specific activity for ATP hydrolysis than the wild-type control, while its K_m for ATP binding remains unchanged. More importantly, the UvrD303 protein unwinds partial duplex DNA up to 10 times more efficiently than wild-type UvrD. The DNA binding affinities of the two proteins appear comparable. Based on these results, we propose that the region located between amino acids 403 and 409 serves to regulate the unwinding activity of DNA helicase II to provide the proper balance between speed and overall effectiveness in the various DNA repair systems in which the protein participates.

Double-stranded DNA needs to be unwound in order for replication, repair, and recombination to proceed. A class of enzymes, designated DNA helicases, accomplish this task by using the energy of nucleoside 5′-triphosphate hydrolysis to disrupt the hydrogen bonds between the Watson-Crick base pairs of duplex DNA. There are at least 12 helicases in *Escherichia coli* (24, 25). One of these, DNA helicase II, the product of the *uvrD* gene, has been demonstrated to play a role in at least two distinct DNA repair pathways: nucleotide excision repair and methyl-directed mismatch repair (29, 39). Analysis of more than a dozen mutant alleles of *uvrD* has suggested that DNA helicase II may also be involved in homologous recombination and replication (5, 12, 53).

DNA helicase II is a single-stranded DNA-dependent ATPase that unwinds double-stranded DNA with a 3′-to-5′ polarity with respect to the DNA strand on which the enzyme initially binds (23). At low protein concentrations, DNA helicase II preferentially unwinds duplex DNA possessing 3′-flanking single-stranded DNA. At much higher concentrations of DNA helicase II, unwinding of blunt-ended or nicked duplex DNA is observed (37). While it has been reported that DNA helicase II is monomeric in solution (1, 35), dimers or oligomers can be formed upon binding DNA (20), and it is proposed that the dimeric helicase is the functionally active form in DNA unwinding (3).

Computer analysis of the *uvrD* coding sequence has indicated that it contains seven conserved motifs that are shared by a superfamily of proteins involved in DNA metabolism (16). Motifs IA, IB, and II, previously identified as Walker A and Walker B sequences, respectively, are conserved segments found in many nucleoside triphosphate-binding proteins and all helicases characterized to date (14, 15, 46). Mutations within these two motifs of DNA helicase II result in proteins with significantly reduced ATP-binding and/or ATP hydrolysis activity (8, 12, 48). In addition, there is genetic evidence that all of the remaining motifs (III to VI) are also required for the biological functions of DNA helicase II (8–10, 51).

While study of the seven conserved motifs can lead to a better understanding of the universal structure-function relationships among this family of proteins, identification of important regions unique to UvrD could help better explain the specialization among DNA helicases and provide a deeper insight into the specific roles of DNA helicase II in vivo. For example, while DNA helicase II and the Rep helicase share 40% homology at the amino acid level (13), the Rep enzyme works catalytically (4), while the UvrD protein is required in stoichiometric amounts (2, 17).

In this communication, we report the identification of a new region of DNA helicase II that is required for in vivo function. Located between amino acids 403 and 409, mutations in this region lead to both temperature-sensitive and dominant phenotypes. Among the five mutant alleles identified, the substitution of two adjacent aspartic acid residues with alanines (*uvrD303*) resulted in a dominant negative phenotype for UV and methyl methanesulfonate (MMS) sensitivity while exhibiting reduced levels of spontaneous mutagenesis and homologous recombination. The purified UvrD303 protein exhibits a higher specific activity for DNA-dependent ATP hydrolysis

* Corresponding author. Mailing address: Department of Genetics, University of Georgia, Athens, GA 30602. Phone: (706) 542-8000. Fax: (706) 542-3910. E-mail: skushner@uga.cc.uga.edu.

† Present address: Memorial Sloan-Kettering Cancer Center, New York, NY 10021.

TABLE 1. Strains used in this work

Strains	Genotype (strain/plasmid)	Source or reference
SK707	F$^-$ *uvrD*$^+$ *rep*$^+$ *argH1 hisG4 ilvD188 metE46 lacMS286*ϕ80dII*lacBK1*	52
SK4090	F$^-$ *uvrD*Δ*294*::*kan*[a] *rep*$^+$ *argH1 hisG4 ilvD188 metE46 lacMS286*ϕ80dII*lacBK1*	51
SK9040	SK4090 transformed with pWSK29 (*uvrD*Δ*294*)	This work
SK9041	SK4090 transformed with pGZK20 (*uvrD*Δ*294*/*uvrD*$^+$)	This work
SK9052	SK4090 transformed with pGZK28 (*uvrD*Δ*294*/*uvrD300*)	This work
SK9053	SK4090 transformed with pGZK29 (*uvrD*Δ*294*/*uvrD301*)	This work
SK9054	SK4090 transformed with pGZK30 (*uvrD*Δ*294*/*uvrD302*)	This work
SK9055	SK4090 transformed with pGZK31 (*uvrD*Δ*294*/*uvrD303*)	This work
SK9056	SK4090 transformed with pGZK32 (*uvrD*Δ*294*/*uvrD304*)	This work
SK9060	SK707 transformed with pWSK29 (*uvrD*$^+$)	This work
SK9061	SK707 transformed with pGZK20 (*uvrD*$^+$/*uvrD*$^+$)	This work
SK9062	SK707 transformed with pGZK28 (*uvrD*$^+$/*uvrD300*)	This work
SK9063	SK707 transformed with pGZK29 (*uvrD*$^+$/*uvrD301*)	This work
SK9064	SK707 transformed with pGZK30 (*uvrD*$^+$/*uvrD302*)	This work
SK9065	SK707 transformed with pGZK31 (*uvrD*$^+$/*uvrD303*)	This work
SK9066	SK707 transformed with pGZK32 (*uvrD*$^+$/*uvrD304*)	This work
SK9067	SK4090 transformed with pGZK33 (*uvrD*Δ*294*/*uvrD*$^+$)	This work
SK9070	SK4090 transformed with pGP1-3	This work
SK9071	SK9071 transformed with pGZK20	This work
SK9072	SK9072 transformed with pGZK31	This work

[a] *uvrD*Δ*294*::*kan* is a complete deletion of the *uvrD* coding sequence replaced by a *kan* cassette. For the sake of simplicity, it is given in the text as *uvrD*Δ*294.*

and unwinds DNA partial duplexes up to 10 times more efficiently than the wild-type DNA helicase II protein. The implications of these results are discussed.

MATERIALS AND METHODS

Strains and plasmids. The *E. coli* strains used in this work are listed in Table 1. All strains were constructed in this laboratory by bacteriophage P1-mediated transduction (50) or plasmid transformation unless otherwise described. The plasmids used are described in Table 2. The various *uvrD* genes were inserted into pWSK29 (47), such that they could be transcribed from a bacteriophage T7 promoter.

Media and growth conditions. Cells were grown in Luria broth (21) unless otherwise described. Ampicillin (100 μg/ml), kanamycin (20 μg/ml), and chloramphenicol (20 μg/ml) were added when necessary. Agar was added to 2% for solid medium. The minimal medium used for P1 transduction was M56/2 (18) containing 2% agar, glucose, and appropriate amino acids and vitamins. Glucose was replaced with lactose (glucose free; Sigma) for lactose minimal medium.

For assays of temperature-sensitive phenotypes, we used 30 and 44°C as the incubation temperatures. Otherwise, the cells were grown at 37°C.

DNA techniques. Plasmid DNA was isolated according to the alkaline lysis method (38) for mini-scale preparations. The Qiagen Midikit from Qiagen was used for larger-scale plasmid preparations. Competent cells were prepared and transformed by electroporation (28) with a Gene Pulser manufactured by Bio-Rad Laboratories, Richmond, Calif.

Random in vivo mutagenesis was carried out as follows: SK9041[pGZK20 (*uvrD*$^+$)] was grown to 10^8 cells per ml in Luria broth followed by the addition of ethyl methanesulfonate (EMS) to 1.5% (vol/vol). Incubation was continued with shaking at 37°C for 2.5 h. Mutagenized plasmid DNA was subsequently extracted and transformed into SK4090 (*uvrD*Δ*294*). The transformants were screened by replica plating (11) for UV sensitivity at 30 and 44°C following exposure to 25 J/m^2 from a General Electric 15-W germicidal lamp. Among 18,000 transformants screened, we isolated 16 nonconditional UV-sensitive mutants and one conditional UV-sensitive mutant (*uvrD300*).

Site-directed mutagenesis was carried out with the U.S.E. Mutagenesis Kit from Pharmacia Biotech. A 2.9-kb *Sal*I DNA fragment containing the *uvrD* gene cloned in pWSK29 (47) was the target for site-directed mutagenesis. The oligonucleotide primers used in this work, with the altered codons underlined, were as follows. Oligonucleotide 5′-CACGCTCAAAGGCCGCGTCGTCGTTGC-3′ was used to revert the *uvrD300* allele to wild type, oligonucleotide 5′-CACGCTCAAAGACCGCGTCGTCGTTGC-3′ was used to alter codon 406 to generate *uvrD301*, oligonucleotide 5′-CACGCTCAAAGGACGCGTCGTCGTTGC-3′ was used to alter codon 406 to generate *uvrD302*, oligonucleotide 5′-CTCAAAGGCCGCGGCGGCGTTGCGGTTG-3′ was used to alter codons 403 and 404 to generate *uvrD303*, and oligonucleotide 5′-CGTATTCACCACAGCCGCAAAGGCCGCGTC-3′ was used to alter codons 408 and 409 to generate *uvrD304.*

All of the mutations were confirmed by DNA sequence analysis. Sequencing was performed with the fmol sequencing system from Promega.

Genetic assays. The UV survival of bacterial strains was measured as described by Zhang et al. (51). MMS sensitivity assays were performed in liquid medium by the method of Siegel (42).

Intrachromosomal recombination was analyzed by measuring the number of *lac*$^+$ revertant colonies resulting from genetic recombination between two partially deleted lactose operons (*lacMS286*ϕ80dII*lacBK1*) in the bacterial chromosome (52). Cells were grown to 10^8 cells per ml in Luria broth and resuspended in M56/2 buffer after being washed twice with the same buffer. Various dilutions were plated on lactose minimal agar plates. Appropriate dilutions were also plated on Luria agar plates to determine the number of viable cells. After 48 h of incubation at 37°C, the numbers of colonies on both sets of plates were counted.

Determination of conjugational recombination frequencies was performed as described by Willetts and Clark (50). SK7712, the Hfr donor, transferred *hisG1* early, while the recipient strains carried a *hisG4* allele. Following a 50-min mating period, cells were vigorously vortexed, washed and resuspended in M56/2

TABLE 2. Plasmids used in this work

Plasmid	Description[a]	Source or reference
pGP1-3	Tc^r plasmid carrying T7 RNA polymerase gene under λ*c*I857 control	44
pWSK29	Ap^r low-copy-number vector	47
pGZK20	Ap^r low-copy-number *uvrD*$^+$ plasmid	*uvrD*$^+$ cloned in *Sal*I site of pWSK29
pGZK28	Ap^r *uvrD300* (A406T) substitution in pGZK20	Isolated by EMS mutagenesis
pGZK29	Ap^r *uvrD301* (A406V) substitution in pGZK20	Site-directed mutagenesis
pGZK30	Ap^r *uvrD302* (A406S) substitution in pGZK20	Site-directed mutagenesis
pGZK31	Ap^r *uvrD303* (D403AD404A) substitution in pGZK20	Site-directed mutagenesis
pGZK32	Ap^r *uvrD304* (E408AR409A) substitution in pGZK20	Site-directed mutagenesis
pGZK33	Ap^r *uvrD*$^+$ (T406A) substitution in pGZK28	Site-directed mutagenesis

[a] Mutationally altered *uvrD* genes were isolated as described in Materials and Methods. The positions of amino acid substitutions are indicated in parentheses.

buffer, and plated onto minimal medium containing the necessary supplements but no histidine. The resulting colonies were counted after 48 h of incubation at 37°C.

Mutation frequencies for the appearance of spectinomycin resistance were determined by the method of Luria and Delbruck (21) employing the modifications of Zhang et al. (51).

DNA and nucleotides. All unlabeled deoxynucleoside triphosphates (dNTPs) and ATP, adenosine-5′-*O*-thiotriphosphate, and bacteriophage M13mp19 were from Boehringer Mannheim. Single- and double-stranded M13 phage DNAs were prepared according to the method described by Yanisch-Perron et al. (34). [γ-^{32}P]ATP (6,000 mCi/μmol) and [α-^{32}P]dCTP (3,000 mCi/μmol) were provided by Dupont.

Protein purification. The UvrD303 and UvrD$^+$ proteins were purified according to the method described by Washburn and Kushner (48) with the following modifications. Six liters of either SK9071 or SK9072 cells was grown at 30°C in Luria-Bertani medium containing 25 μg of kanamycin and 100 μg of ampicillin per ml to an optical density at 595 nm of about 1.5. The T7 RNA polymerase-directed expression of *uvrD* was induced by a 30-min temperature shift to 42°C. After 90 min of additional incubation with shaking at 37°C, cells were collected by centrifugation and frozen as cell paste at −20°C for storage.

Cells were lysed and treated with 30% (wt/vol) ammonium sulfate for protein precipitation as described by Washburn and Kushner (48). The pellet was subsequently redissolved in 400 ml of buffer AP (20 mM potassium phosphate [pH 7.5], 0.1 mM EDTA, 0.5 mM EGTA, 20 mM β-mercaptoethanol, 0.1 mM phenylmethylsulfonyl fluoride [PMSF], 20% [vol/vol] glycerol) as fraction I. Fraction I was applied to a phosphocellulose column (5 by 11 cm [Whatman P11]) equilibrated with buffer AP. After being washed with 500 ml of the same buffer, proteins were eluted with a 0 to 0.5 M NaCl linear gradient (total volume, 500 ml) in buffer AP. Immuno dot blotting and Western blotting were used to detect the *uvrD* gene product. The peak fractions (0.17 M NaCl) were pooled (fraction II) and dialyzed overnight against 2 liters of buffer P (20 mM potassium phosphate [pH 6.5], 0.1 mM EDTA, 0.5 mM EGTA, 20 mM β-mercaptoethanol, 0.1 mM PMSF, 20% [vol/vol] glycerol). The dialyzed fraction II was applied to a phosphocellulose column (2.5 by 10 cm [Whatman P11]) preequilibrated with buffer P. The column was washed with 250 ml of buffer P and eluted with a 0.2 to 1.0 M NaCl linear gradient (total volume, 120 ml) in buffer P. Immunoblotting was performed, and the peak fractions (0.6 M NaCl) were pooled (fraction III) and dialyzed against buffer A (20 mM Tris-HCl [pH 7.5], 0.1 mM EDTA, 0.5 mM EGTA, 20 mM β-mercaptoethanol, 0.1 mM PMSF, 20% [vol/vol] glycerol). The dialyzed fraction III was subsequently applied to a single-stranded DNA agarose column (1.2 by 8 cm [Life Technologies]) and eluted with a 40-ml NaCl linear gradient (0.2 to 1.0 M). The peak fractions (0.6 M NaCl), detected by immunoblotting, were pooled, dialyzed against buffer A containing 50% glycerol, and stored at −20°C (fraction IV). The columns were prepared according to the manufacturers' instructions. Both the UvrD$^+$ and UvrD303 proteins were stable during the process of purification. Protein concentrations were determined with the Bradford assay (7) with bovine serum albumin as the standard.

Immunological methods. For immuno dot blotting, 200 to 400 μl of each fraction was vacuum blotted onto polyvinylidene difluoride Immobilon-P transfer membranes (Millipore) with a Schleicher & Schuell dot blotter. For Western blotting, 15 μl of each fraction was applied to a 10% polyacrylamide gel. After electrophoresis, the proteins in the gel were transferred onto polyvinylidene difluoride transfer membranes as described previously (32). The membranes were probed with anti-UvrD antibodies (48) and developed with an enhanced chemiluminescence (ECL) Western blotting kit from Amersham Life Science. Western blot analysis of the UvrD protein in various mutant strains was carried out as described by Zhang et al. (51).

DNA-dependent ATPase assays. The hydrolysis of ATP to ADP was measured as previously described (19). The standard ATPase reaction mixture (75 μl) contained 50 mM Tris-HCl (pH 7.5), 20 mM β-mercaptoethanol, 3 mM $MgCl_2$, 15 μg of bovine serum albumin, 2.5 μg of heat-denatured calf thymus DNA, [γ-^{32}P]ATP (2×10^4 to 10×10^4 cpm/reaction) and UvrD protein as indicated. For k_{cat} determinations, the ATP concentration was 500 μM. For K_m determinations, the ATP concentration ranged from 2 to 100 μM.

DNA helicase substrate preparation. DNA helicase substrates consisted of single-stranded M13mp19 DNA to which ^{32}P-labeled fragments of various sizes were annealed. The 24-nucleotide oligomer was an M13/pUC forward primer supplied by Promega. It was end labeled with T4 polynucleotide kinase (Boehringer Mannheim) and [γ-^{32}P]ATP and annealed to M13 single-stranded DNA as previously described (48).

The 96- and 448-bp fragments were obtained by digestion of double-stranded M13mp19 DNA with the restriction enzyme *Pvu*II. After electrophoresis, the DNA fragments were recovered from a 1.5% agarose gel, annealed to M13 DNA, and labeled with Klenow DNA polymerase and [α-^{32}P]dCTP as described by Matson (23). Unreacted radioactive nucleotide and the complementary strand of the restriction fragment were removed by gel filtration through a 1.5-ml Sepharose 6B-CL column equilibrated with 10 mM Tris-HCl (pH 7.5)–0.2 mM EDTA–50 mM NaCl. The void volume was used directly in the helicase assays. The 346-bp blunt-ended full duplex substrate was constructed as previously described (12).

DNA helicase assays. The helicase assays measured either the displacement of a ^{32}P-labeled DNA fragment from a single-stranded circular partial duplex or the denaturation of a full duplex ^{32}P-labeled DNA fragment by polyacrylamide gel electrophoresis. Reaction mixtures (20 μl) contained 40 mM Tris-HCl (pH 7.5), 4 mM $MgCl_2$, 1 mM dithiothreitol, 50 μg of bovine serum albumin per ml, 3 mM ATP, and approximately 2 μM DNA substrate (for assays with the 346-bp full duplex DNA fragment, the substrate was approximately 0.5 μM). Reactions were carried out at 37°C for 10 min and terminated by addition of 10 μl of stop solution (50 mM EDTA, 40% glycerol, 0.3% sodium dodecyl sulfate, and 0.03% bromphenol blue). The reaction mixtures were loaded onto 6% nondenaturing polyacrylamide gels. To quantitate unwinding levels, the gels were exposed to X-ray films, which were then scanned on a Molecular Dynamics scanning densitometer. The percentage of unwinding was calculated by the formula $[(U - C)/(B - C)] \times 100$, where U is the intensity (scan units) of the band produced by the unwinding reaction, C is the amount (scan units) of unwound DNA in the absence of the enzyme, and B is the amount (scan units) of unwound DNA produced by heating the reaction mixture at 95°C for 8 min before loading the gel.

DNA-binding assay. A nitrocellulose filter-binding assay was used to measure binding of the UvrD proteins to DNA (26). The binding reaction mixture was identical to the helicase assay reaction mixture, except the ATP was replaced with 3 mM γ-S–ATP. The DNA substrate was the 448-bp partial duplex as described above. The reaction was carried out at 37°C for 10 min, followed by dilution with 1 ml of prewarmed buffer (40 mM Tris-HCl [pH 7.5], 4 mM $MgCl_2$, 1 mM dithiothreitol, 50 μg of bovine serum albumin per ml). The reaction mixtures were then passed through nitrocellulose filters (Whatman [0.45-μm pore diameter]). The filters were subsequently washed three times with 1× 3 ml of reaction buffer before drying. The dried filters were counted in a liquid scintillation counter (Beckman). Background radioactivity was subtracted from the total radioactivity measured.

RESULTS

Identification of a new temperature-sensitive *uvrD* mutation. Historically, the isolation and characterization of temperature-sensitive alleles in the structural gene of a protein involved in multiple pathways has proven useful as a means of helping understand its function. With DNA helicase II playing important roles in excision repair, mismatch repair, and genetic recombination, the *uvrD* gene is a perfect candidate for such an approach. However, although Richet et al. (36) isolated a DNA helicase II protein with temperature-sensitive ATPase activity in vitro, it demonstrated no in vivo phenotype.

Accordingly, we have sought for some time to isolate and characterize new temperature-sensitive *uvrD* alleles by a variety of genetic approaches. As described in Materials and Methods, here we used EMS mutagenesis on a low-copy-number plasmid carrying the *uvrD*$^+$ gene to generate potential temperature-sensitive *uvrD* alleles. After searching through 18,000 individual colonies carrying mutagenized *uvrD* plasmids, we isolated a mutant allele (*uvrD300*) which led to increased UV sensitivity at 44°C. In a host strain with a complete chromosomal deletion of the *uvrD* coding sequence [SK4090 (*uvrDΔ294*)], the UV survival rate of the *uvrD300* mutant decreased significantly at 44°C (Fig. 1). However, the *uvrD300* allele did not fully complement *uvrDΔ294* at 30°C (Fig. 1). In contrast, the presence of the *uvrD*$^+$ allele on the same low-copy-number plasmid led to a small increase in UV resistance at 44°C (Fig. 1). To our surprise, when plasmid pGZK28 (*uvrD300*) was transformed into SK707 (*uvrD*$^+$), we again observed UV sensitivity at both 30 and 44°C (Fig. 1). In fact, at 44°C, the UV sensitivities of SK9052 (*uvrDΔ294*/*uvrD300* [strain/plasmid]) and SK9062 (*uvrD*$^+$/*uvrD300*) were strikingly close.

DNA sequence analysis of the complete *uvrD* gene in pGZK28 revealed a single G-to-A change in the coding region, resulting in the substitution of alanine with threonine at amino acid 406 (A406T). When we subsequently reverted the A to G by using site-directed mutagenesis, the UV sensitivity of the strain carrying pGZK33 was identical to that observed with SK9041(pGZK20 [Fig. 1]).

Identification of a new region required for normal in vivo DNA helicase II function. After determining the exact location

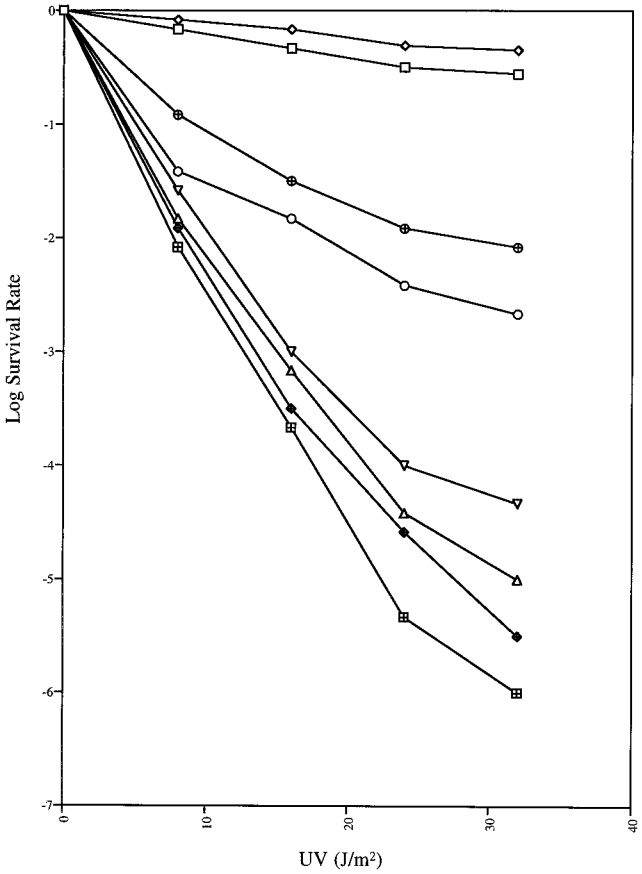

FIG. 1. UV sensitivity of strains carrying the *uvrD300* (A406T) mutation. Experiments were carried out as described in Materials and Methods. Data (log survival) are expressed as the logarithmic function of the number of UV-irradiated cells forming colonies divided by the number of colonies formed by unirradiated cells. Survival curves represent the average of at least three independent determinations. ⊞, SK9040 (*uvrDΔ294*/pWSK29) at 30°C; ◆, SK9040 (*uvrDΔ294*/pWSK29) at 44°C; □, SK9041 (*uvrDΔ294*/*uvrD*$^+$) at 30°C; ◇, SK9041 (*uvrDΔ294*/*uvrD*$^+$) at 44°C; ○, SK9052 (*uvrDΔ294*/*uvrD300*) at 30°C; △, SK9052 (*uvrDΔ294*/*uvrD300*) at 44°C; ⊕, SK9062 (*uvrD*$^+$/*uvrD300*) at 30°C; and ▽, SK9062 (*uvrD*$^+$/*uvrD300*) at 44°C. SK9067 gave survival curves identical to those of SK9041.

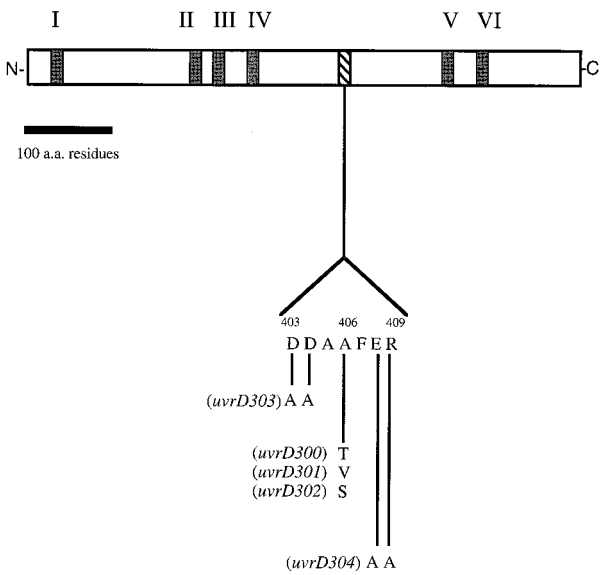

FIG. 2. Schematic representation of DNA helicase II protein sequence. Motifs I to VI, the six conserved regions that are shared by a large family of helicases, including DNA helicase II (16), are indicated. The locations and amino acid sequences of the mutations described in this work are indicated below the diagram. a.a., amino acids.

of the *uvrD300* allele, we realized that it was not located within any of the seven previously identified conserved motifs (16) (Fig. 2). Interestingly, however, we noticed that there were four charged amino acids flanking the alanine (position 406) residue (DDAAFER [Fig. 2]). To determine if these charged amino acids were important for normal biological function, we used the approach of Bennett et al. (6) to change the two aspartic acids to alanine to create *uvrD303* and the glutamic acid and arginine residues to alanine to generate *uvrD304*. In addition, we made two additional substitutions of valine (*uvrD301*) and serine (*uvrD302*) at position 406 (Fig. 2). As judged by Western blot analysis, all of the mutant alleles produced stable UvrD protein in amounts comparable to those of a wild-type control (Fig. 3). Interestingly, the *uvrD302*, *uvrD303*, and *uvrD304* alleles led to small changes in the electrophoretic mobility of the full-length protein (Fig. 3).

The *uvrD301* allele (A406V) also exhibited temperature sensitivity to UV irradiation in the *uvrDΔ294* genetic background (Fig. 4), but consistently resulted in less UV sensitivity than *uvrD300* (Fig. 1). The *uvrD302* allele, on the other hand, appeared to be a neutral mutation (Fig. 5A). In contrast, the *uvrD303* and *uvrD304* alleles showed various levels of increased UV sensitivity (Fig. 5A), which were not affected by temperature (data not shown). The *uvrD303* strain was almost as UV sensitive as a *uvrDΔ294* control (Fig. 5A).

We also investigated the possibility of phenotypic dominance of these mutations by transforming them into SK707, which carried the wild-type *uvrD* allele on the chromosome. Of the five alleles tested, *uvrD300*, *uvrD301*, and *uvrD303* were clearly dominant to the wild-type gene when present in six to eight copies per cell (Fig. 1, 4, and 5B). In contrast, six to eight copies of the wild-type gene did not cause any significant increase in UV sensitivity (Fig. 5B).

MMS sensitivity. Previous studies have shown that the DNA lesions caused by alkylating agents like MMS can be repaired by a pathway that somehow involves DNA helicase II. These mutations in *uvrD* can result in moderate (*uvrDΔ288* [49] and *uvrD252* [48]) or strong (*uvrD3* [43]) MMS sensitivity. To assess the effect of our new *uvrD* mutations in this regard, we measured the viability of the strains harboring each of these mutant *uvrD* alleles in the presence of MMS (Fig. 6). Interest-

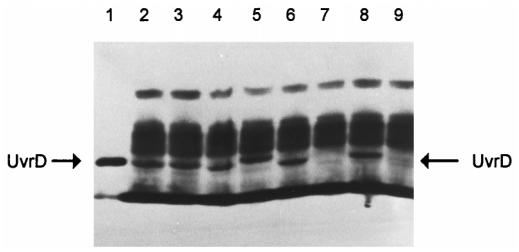

FIG. 3. Western blot analysis of the expression of various *uvrD* alleles. Experiments were carried out as described in Materials and Methods. Lanes: 1, 75 ng of purified UvrD$^+$ protein; 2 to 9, 15 μg of total cell protein from strains carrying various *uvrD* alleles as follows: 2, SK9052 (*uvrD300*); 3, SK9053 (*uvrD301*); 4, SK9054 (*uvrD302*); 5, SK9055 (*uvrD303*); 6, SK9056 (*uvrD304*); 7, SK9040 (*uvrDΔ294::*Kan^r); 8, SK9041 (*uvrD*$^+$); 9, SK707 (*uvrD*$^+$).

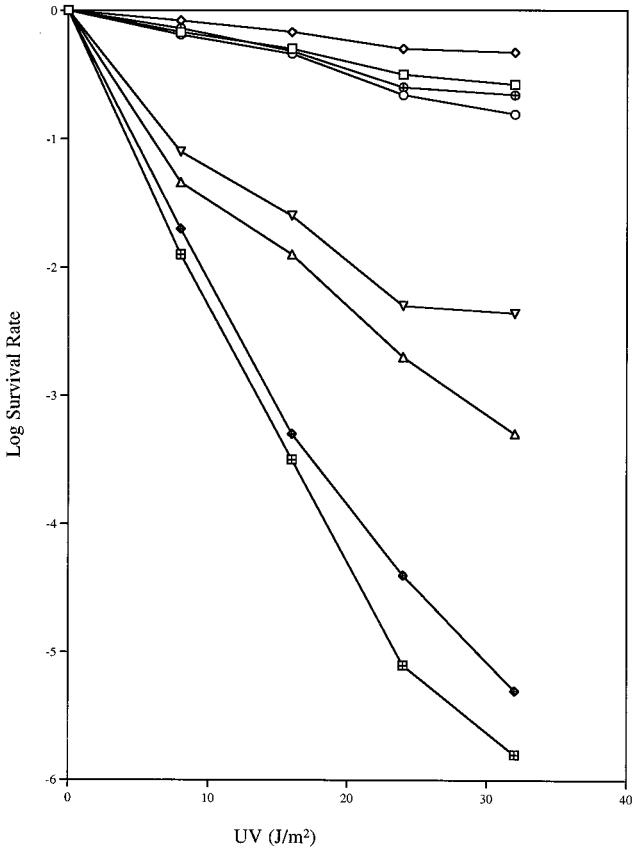

FIG. 4. UV sensitivity of strains carrying the *uvrD301* (A406V) mutation. Experiments were carried out as described in Materials and Methods. Data (log survival) are expressed as the logarithmic function of the number of UV-irradiated cells forming colonies divided by the number of colonies formed by unirradiated cells. The data presented represent the average of at least three independent experiments. ⊞, SK9040 (*uvrDΔ294*/pWSK29) at 30°C; ◆, SK9040 (*uvrDΔ294*/pWSK29) at 44°C; □, SK9041 (*uvrDΔ294*/*uvrD*$^+$) at 30°C; ◇, SK9041 (*uvrDΔ294*/*uvrD*$^+$) at 44°C; ○, SK9053 (*uvrDΔ294*/*uvrD301*) at 30°C; △, SK9053 (*uvrDΔ294*/*uvrD301*) at 44°C; ⊕, SK9063 (*uvrD*$^+$/*uvrD301*) at 30°C; and ▽, SK9062 (*uvrD*$^+$/*uvrD301*) at 44°C.

ingly, although *uvrD300* and *uvrD301* were temperature sensitive in the UV sensitivity assay (Fig. 1 and 4), their MMS sensitivity was temperature independent (data not shown) and was similar to that of a *uvrDΔ294*/*uvrD*$^+$ control (Fig. 6).

As previously reported for more limited deletions of the *uvrD* coding sequence (49), the *uvrDΔ294* strain (SK9040) exhibited an increase in MMS sensitivity (Fig. 6). However, the presence of the *uvrD303* allele in the *uvrDΔ294* genetic background significantly increased the MMS sensitivity (Fig. 6). This result is in contrast to those of the UV sensitivity tests, in which the presence of *uvrD303* in the *uvrDΔ294* background led to slightly decreased resistance (Fig. 5A). In addition, when pGZK31 (*uvrD303*) was transformed into SK707 (*uvrD*$^+$), the MMS sensitivity of the resulting strain (SK9065) was also greater than that of the *uvrDΔ294* strain (Fig. 6).

Spontaneous mutation frequencies. DNA helicase II is known to be required in the methyl-directed DNA mismatch repair pathway (29). Its functional inactivation results in increased frequencies of spontaneous mutagenesis (49). However, although most of the previously reported *uvrD* alleles result in increased UV sensitivity, the *uvrD3* and *uvrD252* alleles do not increase spontaneous mutation rates (43, 48). These observations suggest that DNA helicase II might play different roles in mismatch repair versus excision repair. Since our new *uvrD* alleles displayed interesting phenotypes regarding excision repair (Fig. 1, 4, and 5), we also tested the effect of these mutants on the mismatch repair pathway. As a test for increased levels of spontaneous mutagenesis, we measured the appearance of spectinomycin-resistant cells, as described in Materials and Methods. In agreement with previous results with partial deletion mutants (49), the complete deletion of the *uvrD* coding sequence (*uvrDΔ294*) resulted in an almost 250-fold increase in spontaneous mutations (Table 3). Of the five new alleles tested, *uvrD300* and *uvrD302* were neutral, while *uvrD301*, *uvrD303*, and *uvrD304* led to 5- to 10-fold reductions in mutation frequencies, suggesting a strong antimutator effect for these alleles.

Homologous recombination. Beyond its well-documented roles in DNA repair pathways, *uvrD* has also been implicated in homologous recombination by a series of genetic and biochemical studies (5, 22, 27, 30). A *uvrD* null mutant exhibited a hyperrecombination phenotype (49), which fit the hypothesized role of DNA helicase II in the proposed antirecombinase model (33, 34). However, the details of UvrD function in this process have not been well defined. Moreover, at least one *uvrD* allele (*uvrD3*) showed no effect on recombination frequency, although it severely inhibited excision repair (53).

It was therefore of interest to determine if our newly isolated mutant alleles affected recombination rates. We employed two different systems to measure homologous recombination. One was to test conjugational recombination by using genetic markers transferred from an Hfr strain (50). The other was to measure the appearance of *lac*$^+$ recombinants formed by intrachromosomal recombination between two partially deleted lactose operons (52). The results, summarized in Tables 4 and 5, indicate that these mutations do not increase homologous recombination in the cells when present at six to eight copies per cell. In fact, the *uvrD303* allele led to a 10-fold reduction in conjugal recombination (Table 4) and a 2-fold decrease in intrachromosomal recombination (Table 5).

Purification of UvrD$^+$ and UvrD303 proteins. A 2.9-kb *Sal*I DNA fragment containing either the wild-type *uvrD* gene or *uvrD303* was cloned into a low-copy-number vector, pWSK29 (47), to generate plasmids pGZK20 and pGZK31 (Table 2). The direction of the insertion was selected so that the *uvrD* gene was under the control of a bacteriophage T7 promoter from the vector. For purposes of protein amplification, a *uvrDΔ294*::*kan* strain (51) containing the plasmid carrying T7 RNA polymerase under the control of λ*c*1857 (pGP1-3) was transformed with either pGZK20 (*uvrD*$^+$) or pGZK31 (*uvrD303*). The cells were grown as described in Materials and Methods. Following a 30-min induction at 42°C, the cells were incubated for another 90 min with shaking at 37°C prior to harvesting. The UvrD$^+$ and UvrD303 proteins were purified to greater than 95% homogeneity based on silver staining (Fig. 7), as described in Materials and Methods. Both the wild-type and mutant proteins were detected on the basis of immunoreactivity during the purification process. Interestingly, the purified UvrD303 protein migrated slightly slower in the sodium dodecyl sulfate-polyacrylamide gel (Fig. 7). This result confirmed a similar observation made in crude extracts (Fig. 3). The purified UvrD303 protein was stable for up to 6 months under the storage conditions described above.

ATPase activity. The ATPase assays were performed as described in Materials and Methods. For specific activity determinations, the ATP concentration was 500 μM and the UvrD protein concentration ranged between 0.2 and 20 nM. For K_m determinations, the ATP concentration ranged between 20 and

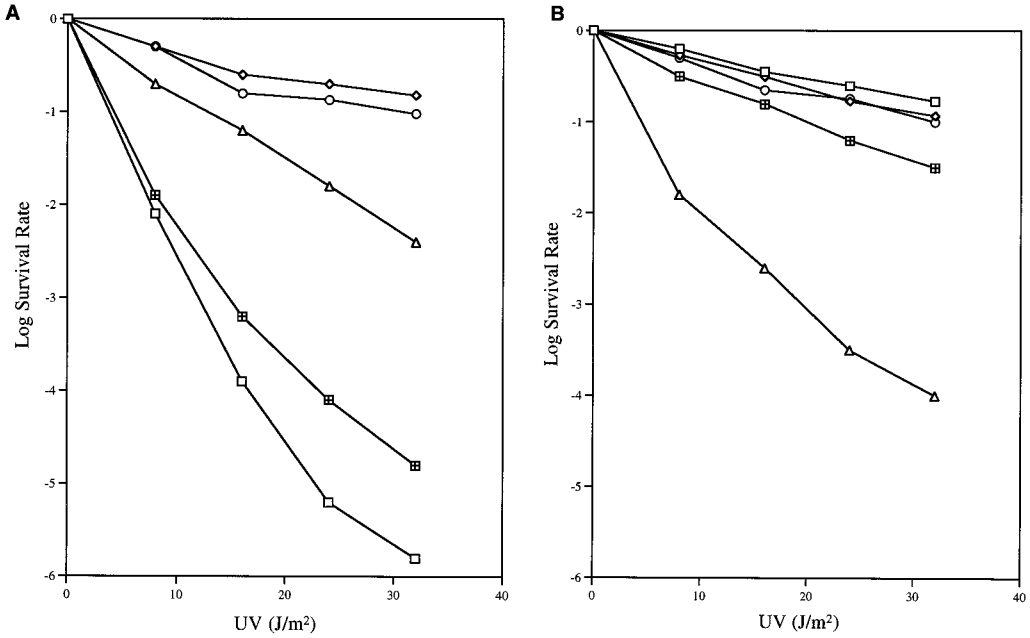

FIG. 5. UV sensitivity of various *uvrD* strains. Experiments were carried out at 37°C as described in Materials and Methods. Data (log survival) are expressed as the logarithmic function of the number of UV-irradiated cells forming colonies divided by the number of colonies formed by unirradiated cells. (A) □, SK9040 (*uvrDΔ294*/pWSK29); ◇, SK9041 (*uvrDΔ294*/*uvrD*$^+$); ○, SK9054 (*uvrDΔ294*/*uvrD302*); ⊞, SK9055 (*uvrDΔ294*/*uvrD303*); △, SK9056 (*uvrDΔ294*/*uvrD304*). (B) □, SK707 (*uvrD*$^+$); ◇, SK9061 (*uvrD*$^+$/*uvrD*$^+$); ○, SK9064 (*uvrD*$^+$/*uvrD302*); △, SK9065 (*uvrD*$^+$/*uvrD303*); ⊞, SK9066 (*uvrD*$^+$/*uvrD304*).

500 μM and the UvrD concentration was 1.1 nM. The non-DNA-dependent ATPase activity was typically less than 5% and was subtracted from the total measurement. As shown in Table 6, the k_{cat} for ATP hydrolysis by the UvrD303 mutant protein was approximately 129 (s^{-1}), a 60% increase compared with the result for wild-type protein, which had a k_{cat} value of 81 (s^{-1}). In contrast, there was no significant difference for the K_m values between the two proteins (Table 6), indicating that the nucleotide binding ability was not affected by the mutation. The specific activity (656 U/μg) and K_m (55 μM) of the wild-type UvrD were in excellent agreement with previous reports (48).

DNA helicase activity. We subsequently compared the unwinding activity of the UvrD303 and UvrD$^+$ proteins by using various partially duplex DNA molecules. The DNA substrates, prepared by annealing of radiolabeled complementary single-stranded DNA oligomers to single-stranded covalently closed M13 DNA as described in Materials and Methods, were incubated with either UvrD$^+$ or UvrD303 proteins. Subsequently the reaction mixtures were separated on 6% nondenaturing polyacrylamide gels (Fig. 8). Under the conditions specified in Materials and Methods, 0.58 ng (0.36 nM) of wild-type UvrD protein was required to produce 50% unwinding of a 24-bp duplex, while only 0.17 ng (0.10 nM) of UvrD303 protein was needed to achieve the same level of unwinding (Fig. 9A).

The enhanced unwinding activity of the UvrD303 protein was also observed with 96- and 448-bp DNA partial duplexes (Fig. 9B and C). Of particular interest was the fact that for the longer substrates, the UvrD303 protein exhibited a higher increase in unwinding activity relative to the wild-type protein. For instance, it required 1.6 ng (1.0 nM) of UvrD303 to unwind 50% of the 96-bp partial duplex substrate, while 13 ng (8.1 nM) of UvrD$^+$ protein was required to unwind the same amount of DNA substrate (Fig. 9B). With the 448-bp partial duplex DNA, 50% unwinding required 6.1 ng (3.8 nM) of UvrD303 versus 60 ng (38 nM) of UvrD$^+$ (Fig. 9C). These data indicated that the UvrD303 protein unwound partial duplex DNA up to 10 times more efficiently than the wild-type UvrD enzyme.

Previous work has shown that at higher UvrD protein concentrations, blunt-ended duplex DNA can be unwound (37). Employing a 346-bp blunt-ended duplex DNA molecule (12), we observed that both the wild-type UvrD and UvrD303 proteins were able to initiate unwinding of the substrate. It required 24 ng (15 nM) of UvrD303 protein to achieve 10% unwinding, while 122 ng (75 nM) of wild-type protein was required for the same effect (data not shown).

UvrD303 retains DNA-binding ability. Since the UvrD303 protein exhibited both higher ATPase and helicase activities than wild-type UvrD, the increased UV and MMS sensitivity observed in strains carrying *uvrD303* (Fig. 5 and 6) could not be explained simply by the loss of DNA helicase II activity. However, the deficiency in excision repair in *uvrD303* strains could possibly be the result of altered DNA-binding affinity. If the mutant protein fails to bind to the DNA substrate, it will not be able to carry out its function to unwind DNA and turn over UvrC protein. Alternatively, if the mutant protein binds at the damage site with exceptionally high affinity, it may physically interfere with the access of DNA polymerase I or DNA ligase to the substrate. Either way, the excision repair process could be aborted. To address these possibilities, we conducted a nitrocellulose filter-binding assay to compare the binding of the two proteins to a partial-duplex DNA substrate. The reaction was carried out as described in Materials and Methods. The results, shown in Fig. 10, demonstrate similar overall DNA binding characteristics for the wild-type and UvrD303 proteins.

DISCUSSION

uvrD, the gene encoding DNA helicase II in *E. coli*, is involved in multiple DNA metabolic pathways, including excision repair, mismatch repair, and homologous recombination. Consequently, it has not been surprising that the phenotypes of

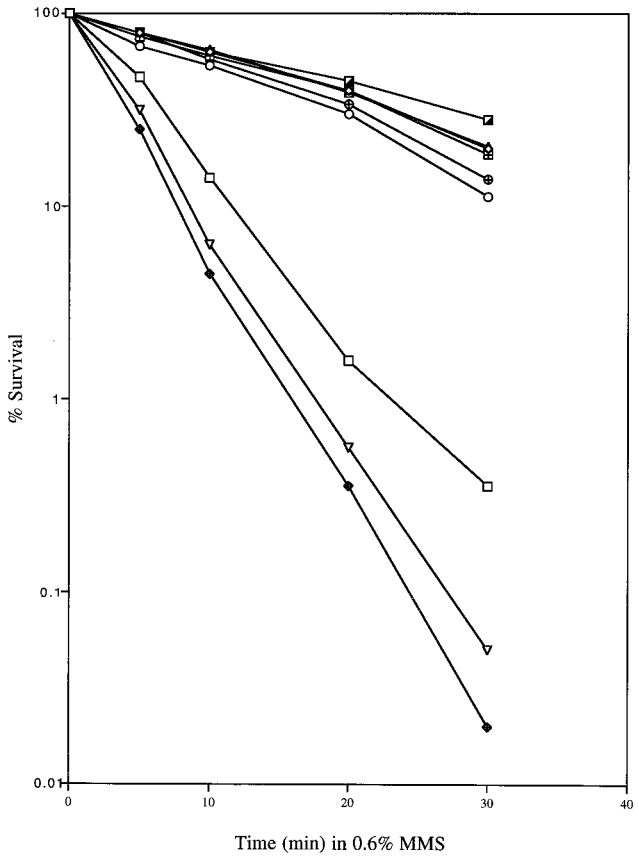

FIG. 6. MMS sensitivity of various strains. The MMS sensitivity assay was performed at 37°C as described in Materials and Methods. Data (percent survival) are expressed as the percentage of MMS-exposed cells forming colonies versus that of unexposed cells forming colonies. □, SK9040 (*uvrDΔ294*/pWSK29); ○, SK9052 (*uvrDΔ294*/*uvrD300*); △, SK9053 (*uvrDΔ294*/*uvrD301*); ⊞, SK9054 (*uvrDΔ294*/*uvrD302*); ◆, SK9055 (*uvrDΔ294*/*uvrD303*); ⊕, SK9056 (*uvrDΔ294*/*uvrD304*); ▽, SK9065 (*uvrD*$^+$/*uvrD303*); ◪, SK9060 (*uvrD*$^+$/pWKS29).

various *uvrD* alleles have sometimes differed (41, 43). Isolation and characterization of new *uvrD* alleles with distinct phenotypes can help to dissect the biological function of the UvrD protein in each pathway and to further understanding of its role in vivo.

Here we have used random mutagenesis in the *uvrD* coding region to generate a mutation resulting in a temperature-sensitive phenotype for UV survival. The location of the mutation site (A406T) was of considerable interest, because it did not fall into any of the seven conserved motifs described by Hodgman (16) (Fig. 2). When we introduced other amino acid substitutions in the region of amino acids 403 to 409, we generated a series of alleles that exhibited a range of phenotypes (Fig. 1 and 4 to 6 and Tables 3 to 5) distinct from that of a *uvrD* null mutation, and from most of the other previously characterized *uvrD* alleles. All of the mutants produced stable UvrD protein (Fig. 3).

The first distinctive feature of mutations in this region is that they exhibit differential UV sensitivities, and all of them except *uvrD302* (A406S) are dominant to the *uvrD*$^+$ allele when present at six to eight copies per cell (Fig. 1, 4, and 5). Interestingly, although they exhibited various levels of UV sensitivity (Fig. 1, 4, and 5), they showed no significant change in sensitivity to MMS, with the exception of *uvrD303* (D403AD404A). In this case, MMS sensitivity was more pronounced than that of *uvrD* deletion strains (Fig. 6). The exceptionally strong increase in MMS sensitivity associated with *uvrD303* suggests that a gain of function, rather than protein interaction, could be responsible for this unusual phenomenon.

TABLE 3. Mutation frequencies in various *uvrD* mutants

Strain	Genotype	Mutation frequency (10^{-10})[a]	Relative mutability[b]
SK707	*uvrD*$^+$	1.9 ± 1.1	1.0
SK9040	*uvrDΔ294*/pWSK29	490 ± 230	258
SK9041	*uvrDΔ294*/pGZK20 (*uvrD*$^+$)	1.3 ± 0.6	0.7
SK9052	*uvrDΔ294*/pGZK28 (*uvrD300*)	2.4 ± 0.1	1.3
SK9053	*uvrDΔ294*/pGZK29 (*uvrD301*)	0.39 ± 0.05	0.2
SK9054	*uvrDΔ294*/pGZK30 (*uvrD302*)	1.8 ± 0.4	1.0
SK9055	*uvrDΔ294*/pGZK31 (*uvrD303*)	0.37 ± 0.02	0.2
SK9056	*uvrDΔ294*/pGZK32 (*uvrD304*)	0.27 ± 0.13	0.1

[a] Mutation frequencies for spectinomycin resistance were calculated by dividing the number of colonies growing on each spectinomycin plate by the number of total cells originally applied to the plate. The data are presented as the average of three independent experiments. All experiments were performed at 37°C as described in Materials and Methods. The viabilities of all the strains tested were identical within the experimental error.

[b] Relative mutability was calculated by comparing the average mutation frequency with that of strain SK707 (*uvrD*$^+$).

Another feature of these mutations is that they seem to retain the biological activity required for successful mismatch repair. Their normal or even lower spontaneous mutation frequency compared to that of the wild-type strain (Table 3) demonstrates that none of them can be classified as mutator, a phenotype which is associated with Δ*uvrD* and most other *uvrD* alleles (41–43, 49). In fact, the *uvrD301*, *uvrD303*, and *uvrD304* alleles all showed a strong antimutator phenotype, with 5- to 10-fold reductions in spontaneous mutation frequency for spectinomycin resistance (Table 3). Although it remains to be tested whether this kind of decrease in mutation frequency can be observed at other genetic loci, the results clearly suggest that the mutant proteins may increase the efficiency of mismatch repair.

Equally striking, the mutants we describe here showed no hyperrecombination phenotype. In fact, some of the mutants had significantly lower recombination frequencies than that of a *uvrD*$^+$ strain (Tables 4 and 5). It has been proposed that the methyl-directed mismatch repair system functions as an antirecombinase (33), causing recombination to be aborted if the

TABLE 4. Conjugal recombination in various *uvrD* mutants

Strains	Genotype	No. of *his*$^+$ recombinants/ml	Relative recombination proficiency[a]
SK707	*uvrD*$^+$	$(5.1 \pm 0.7) \times 10^3$	1.0
SK9040	*uvrDΔ294*/pWSK29	$(8.5 \pm 0.7) \times 10^4$	16.9
SK9041	*uvrDΔ294*/pGZK20 (*uvrD*$^+$)	$(3.0 \pm 0.7) \times 10^3$	0.6
SK9052	*uvrDΔ294*/pGZK28 (*uvrD300*)	$(1.5 \pm 0.1) \times 10^3$	0.3
SK9053	*uvrDΔ294*/pGZK29 (*uvrD301*)	$(1.3 \pm 0.3) \times 10^3$	0.3
SK9054	*uvrDΔ294*/pGZK30 (*uvrD302*)	$(2.9 \pm 0.5) \times 10^3$	0.6
SK9055	*uvrDΔ294*/pGZK31 (*uvrD303*)	$(0.5 \pm 0.4) \times 10^3$	0.1
SK9056	*uvrDΔ294*/pGZK32 (*uvrD304*)	$(2.4 \pm 0.7) \times 10^3$	0.5

[a] Recombination assays were performed at 37°C as described in Materials and Methods. Relative recombination proficiency is determined as the recombination frequency divided by that of SK707 (*uvrD*$^+$). Data represent the average of three independent experiments. The viabilities of all of the strains tested were identical within the experimental error.

TABLE 5. Intrachromosomal recombination in various *uvrD* mutants

Strain	Genotype	No. of *lac*$^+$ recombinants/plate	Relative recombination proficiency[a]
SK707	*uvrD*$^+$	76 ± 10	1.0
SK9040	*uvrD*Δ*294*/pWSK29	502 ± 35	6.4
SK9041	*uvrD*Δ*294*/pGZK20 (*uvrD*$^+$)	96 ± 16	1.2
SK9052	*uvrD*Δ*294*/pGZK28 (*uvrD300*)	70 ± 14	0.9
SK9053	*uvrD*Δ*294*/pGZK29 (*uvrD301*)	84 ± 18	1.1
SK9054	*uvrD*Δ*294*/pGZK30 (*uvrD302*)	108 ± 24	1.4
SK9055	*uvrD*Δ*294*/pGZK31 (*uvrD303*)	42 ± 16	0.5
SK9056	*uvrD*Δ*294*/pGZK32 (*uvrD304*)	50 ± 19	0.6

[a] Recombination tests were performed as described in Materials and Methods. Equal amounts of cells for each strain were plated (approximately 10^7 cells/plate) on lactose minimal plates. All experiments were conducted at 37°C. The viabilities of all of the strains tested were identical within the experimental error.

invading strand contains mismatches (34). Thus, a dysfunctional mismatch repair system caused by defective UvrD results in not only increased spontaneous mutagenesis, but also an increase in the frequency of homologous recombination, which is observed in most *uvrD* mutant strains (5, 49, 51). In other words, there is a correlation between a mutator phenotype and an increased level of genetic recombination in *uvrD* mutants. Our results support this hypothesis from the opposite perspective. Namely, if a *uvrD* mutation does not impair mismatch repair, it also has no effect on DNA homologous recombination. Furthermore, the observation of antimutator and hyporecombination phenotypes for the *uvrD303* and *uvrD304* alleles (Tables 4 and 5) suggests that these two mutant proteins lead to an increased efficiency of the mismatch repair pathway, and consequently a reduction in homologous recombination.

The purification of the UvrD303 mutant protein has enabled us to quantitatively characterize its enzymatic properties and deduce the effect of the mutation on its biological functions.

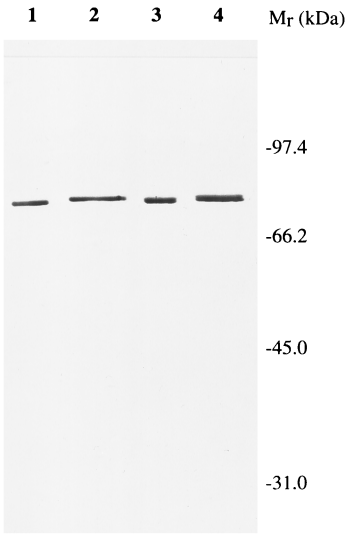

FIG. 7. Silver-stained 6% polyacrylamide–sodium dodecyl sulfate gel of purified UvrD proteins. Wild-type and mutant proteins were purified as described in Materials and Methods. Lanes 1 and 3 represent 250 and 500 ng of wild-type UvrD protein, respectively. Lanes 2 and 4 represent 300 and 600 ng of UvrD303 protein, respectively. The marker proteins used were phosphorylase *b* (97 kDa), bovine serum albumin (66 kDa), ovalbumin (45 kDa), and bovine carbonic anhydrase (31 kDa).

TABLE 6. DNA-dependent ATPase activities of wild-type and mutant UvrD protein

Enzyme	Sp act (U/μg)[a]	k_{cat} (s^{-1})	K_m (μM)
UvrD$^+$	656 ± 29	81 ± 4	55 ± 5
UvrD303	888 ± 71	129 ± 11	59 ± 8

[a] The unit for specific activity is defined as the amount of protein hydrolyzing 1 nmol of ATP in 10 min at 37°C.

What is truly remarkable about the UvrD303 protein is that it actually is both a better ATPase and a better helicase than the wild-type UvrD control. Increased efficiency of unwinding (up to 10-fold) becomes more apparent with longer substrates (Fig. 9) and is even observed with blunt-ended DNA substrates. Furthermore, the data described here provide biochemical support that this region (amino acids 403 to 409) represents a unique feature of DNA helicase II that is critical for both helicase and ATPase activities. This portion of the protein may play some type of regulatory role in maintaining a balance between the unwinding efficiency of the protein versus the optimization of the complex systems (excision repair and mismatch repair) in which it participates.

For most *uvrD* mutants, increased UV sensitivity can be easily explained by the impairment of the excision repair pathway caused by the loss or reduced ATPase or helicase activity associated with the mutant proteins. We initially thought the same explanation would apply to the *uvrD303* allele, which exhibits a significant increase in UV and MMS sensitivity (Fig. 5 and 6). Since UvrD proteins are thought to usually function as dimers (12), the apparent dominance of the mutant allele could result from forming nonfunctional heteromultimers. However, the characterization of UvrD303 protein indicates that it is a hyperactive enzyme, with both enhanced ATPase and helicase activities (Table 6 and Fig. 9). These results effectively rule out the possibility that the observed phenotype arises from the formation of nonfunctional heteromultimers. What are possible hypotheses to explain the increase in UV and MMS sensitivity associated with the *uvrD303* allele?

It should be noted that most models of DNA excision repair in *E. coli* propose that DNA helicase II is only required in the postincision step (39). The suggested function for DNA helicase II is to remove the incised DNA oligomer and turn over the UvrB and UvrC proteins. It has been reported that DNA

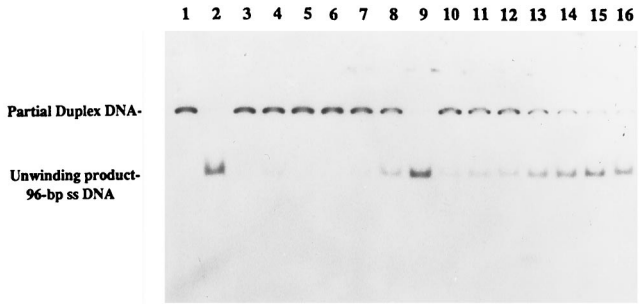

FIG. 8. UvrD303 protein exhibits a higher helicase activity in unwinding partial duplex DNA substrate. Helicase assays were performed as described in Materials and Methods with the 96-bp partial duplex DNA. Reactions were carried out at 37°C. A no-enzyme control was also incubated at the same temperature for the same period of time as the other samples. The fully denatured control was heated at 100°C for 8 min before loading of the samples. Lanes: 1, no-UvrD control; 2, fully heat-denatured DNA; 3 to 9 (UvrD$^+$), 0.32, 0.8, 1.6, 3.2, 6.4, 8.0, and 32 ng, respectively; 10 to 16 (UvrD303), 0.16, 0.32, 0.8, 1.6, 2.4, 3.2, and 6.4 ng, respectively.

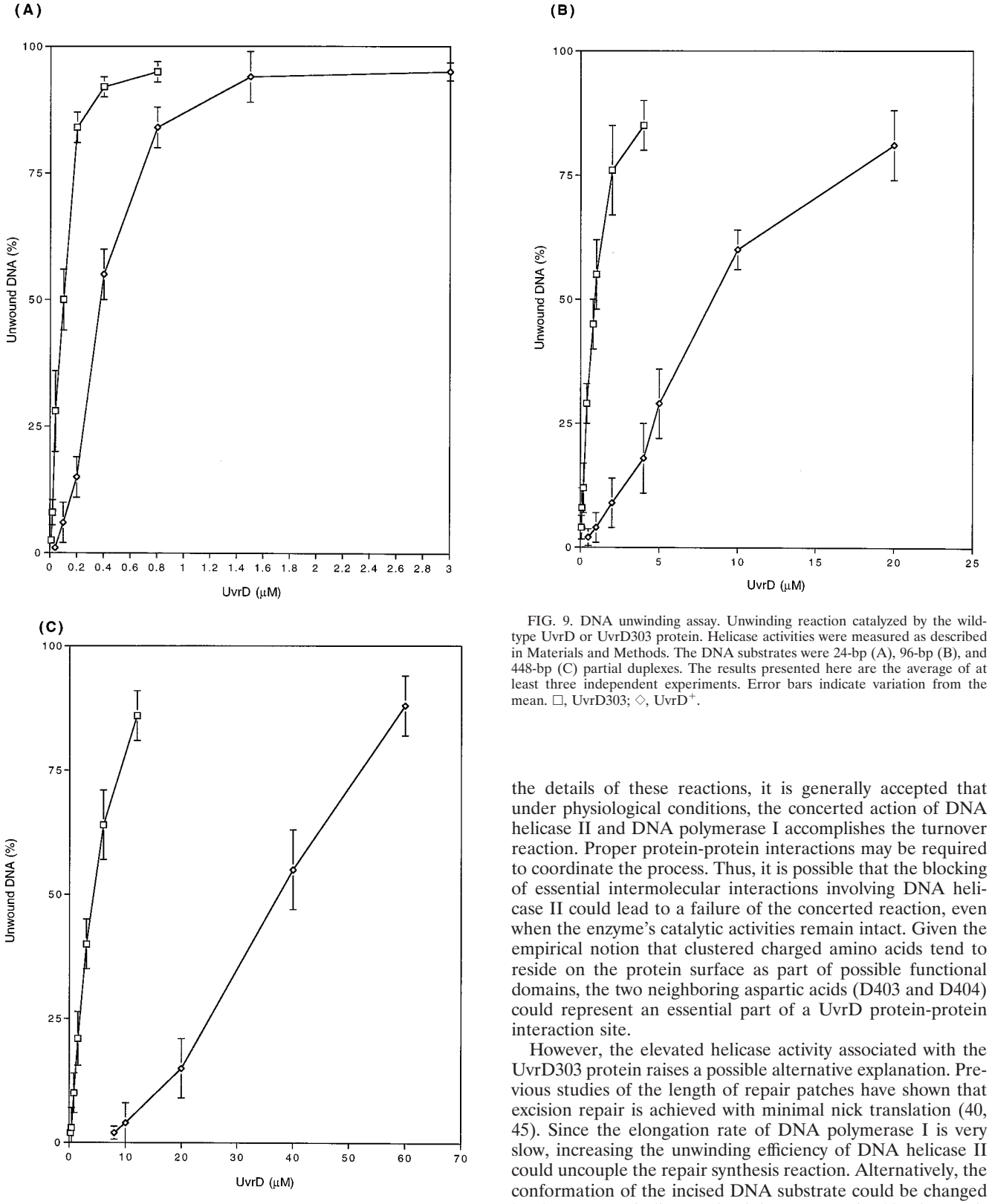

FIG. 9. DNA unwinding assay. Unwinding reaction catalyzed by the wild-type UvrD or UvrD303 protein. Helicase activities were measured as described in Materials and Methods. The DNA substrates were 24-bp (A), 96-bp (B), and 448-bp (C) partial duplexes. The results presented here are the average of at least three independent experiments. Error bars indicate variation from the mean. □, UvrD303; ◇, UvrD$^+$.

helicase II alone is enough to release the photoproduct-containing oligonucleotide and the UvrC protein, while DNA polymerase I is necessary to begin resynthesis and turn over the UvrB protein (31). Although there is some disagreement about the details of these reactions, it is generally accepted that under physiological conditions, the concerted action of DNA helicase II and DNA polymerase I accomplishes the turnover reaction. Proper protein-protein interactions may be required to coordinate the process. Thus, it is possible that the blocking of essential intermolecular interactions involving DNA helicase II could lead to a failure of the concerted reaction, even when the enzyme's catalytic activities remain intact. Given the empirical notion that clustered charged amino acids tend to reside on the protein surface as part of possible functional domains, the two neighboring aspartic acids (D403 and D404) could represent an essential part of a UvrD protein-protein interaction site.

However, the elevated helicase activity associated with the UvrD303 protein raises a possible alternative explanation. Previous studies of the length of repair patches have shown that excision repair is achieved with minimal nick translation (40, 45). Since the elongation rate of DNA polymerase I is very slow, increasing the unwinding efficiency of DNA helicase II could uncouple the repair synthesis reaction. Alternatively, the conformation of the incised DNA substrate could be changed by aberrant unwinding, so that it is not recognized by the repair machinery. Additional experiments will be necessary to test these hypotheses.

Of particular interest is the fact that the *uvrD303* allele actually decreased the frequency of both spontaneous mu-

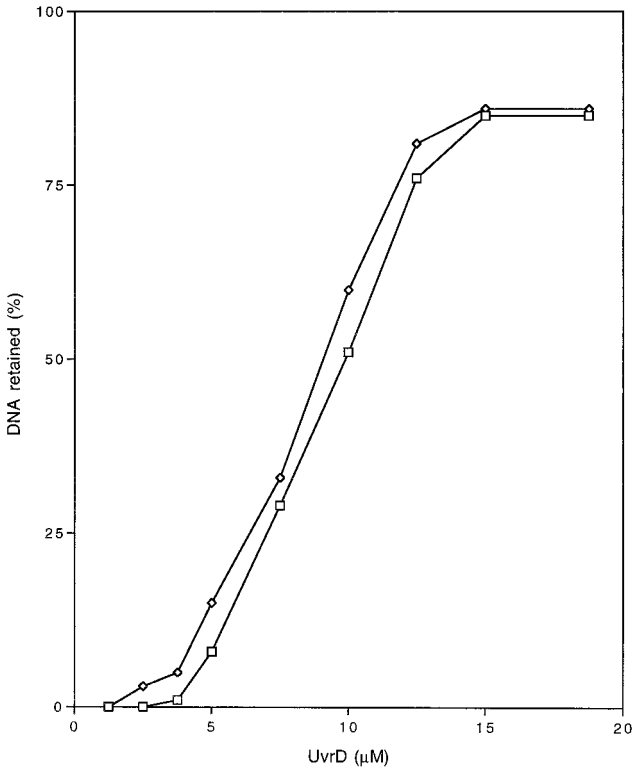

FIG. 10. DNA binding assay. The binding assay was performed as described in Materials and Methods. The percentage of DNA retained is calculated by dividing the radioactivity on the filter by the total radioactivity in each reaction mix. These data represent the average of three independent experiments. □, UvrD303; ◇, UvrD$^+$.

tagenesis and genetic recombination (48), contrary to most other *uvrD* alleles, including *uvrD* deletion alleles (8, 10, 42, 43, 49, 51). This observation suggests that UvrD303 may increase the efficiency of mismatch repair, which is at odds with its effect on excision repair. However, although the unwinding activity of DNA helicase II is presumed to be required in both excision repair and mismatch repair pathways, the other proteins involved in these two processes are different. For example, DNA polymerase III, which is responsible for DNA resynthesis in mismatch repair, is much faster and more processive than DNA polymerase I and should be capable of keeping up with the rapid unwinding associated with UvrD303 protein. In addition, the MutS and MutL proteins, which remain bound at the mismatch site and have unknown function after the incision step (29), might be able to prevent the overunwinding of UvrD303. Consequently, the higher efficiency of mismatch repair observed in *uvrD303* strains (Table 3) could arise from the increased rate of displacement of the incised DNA strand from the GATC site to the actual mismatch.

Although the precise role of UvrD in homologous genetic recombination is not yet defined, it has been proposed that the methyl-directed mismatch repair system acts as an antirecombinase, causing recombination to be aborted if the invading strand contains mismatches (33, 34). In this process, the unwinding activity of DNA helicase II is required for uncoupling the invading strand. This model is supported by the fact that the elimination of DNA helicase II protein or its enzymatic activity results in elevated spontaneous mutation and recombination frequencies within the cell (49). Our results support the antirecombinase model by showing that enhanced unwinding efficiency leads to reduced levels of both spontaneous mutagenesis and homologous recombination.

In conclusion, the use of both random and site-directed mutagenesis has revealed a new region in the *uvrD* coding sequence that is unique to this helicase and is required for normal biological function. Mutations in amino acids 403 to 409 exhibit distinctive phenotypes that are different from the properties associated with most *uvrD* mutant alleles. Since DNA helicase II is involved in multiple pathways of DNA metabolism, mutations in *uvrD* usually generate pleiotropic phenotypes that are difficult to interpret. Isolation of *uvrD* mutants such as these can facilitate the dissection of functions of DNA helicase II, as well as the elucidation of the specific role it plays in each pathway. The results obtained with the mutants we describe here suggest that there are different UvrD functions required in excision repair and mismatch repair.

ACKNOWLEDGMENTS

We thank Stanley Tabor for his generous gift of plasmid pGP1-3, Valerie F. Maples for helpful technical advice, Caroline Ingle and Eileen O'Hara for critically reading the manuscript, and members of this laboratory for stimulating discussions.

This work was partly supported by NIH grants (GM27997 and GM28760) to S.R.K.

REFERENCES

1. **Abdel-Monem, M., M.-C. Chanal, and H. Hoffman-Berling.** 1977. DNA unwinding enzyme II of *Escherichia coli*. 1. Purification and characterization of the ATPase activity. Eur. J. Biochem. **79:**33–38.
2. **Abdel-Monem, M., H. Durwald, and H. Hoffman-Berling.** 1977. DNA unwinding enzyme II of *Escherichia coli*. 2. Characterization of the DNA unwinding activity. Eur. J. Biochem. **79:**39–45.
3. **Ali, J. A., and T. M. Lohman.** 1997. Kinetic measurement of the step size of DNA unwinding by *Escherichia coli* UvrD helicase. Science **275:**377–380.
4. **Arai, N., and A. Kornberg.** 1981. Rep protein as a helicase in an active, isolatable replication fork of duplex ϕX174 DNA. J. Biol. Chem. **256:**5294–5298.
5. **Arthur, H. M., and R. G. Lloyd.** 1980. Hyper-recombination in *uvrD* mutants of *Escherichia coli* K-12. Mol. Gen. Genet. **180:**185–191.
6. **Bennett, W. F., N. F. Paoni, B. A. Keyt, D. Botstein, A. J. Jones, L. Presta, F. M. Wurm, and M. J. Zoller.** 1991. High resolution analysis of functional determinants on human tissue-type plasminogen activator. J. Biol. Chem. **266:**5191–5201.
7. **Bradford, M. M.** 1976. A rapid and sensitive method for the quantitation of microgram quantities of protein utilizing the principle of protein-dye binding. Anal. Biochem. **72:**248–254.
8. **Brosh, R. M., Jr., and S. W. Matson.** 1995. Mutations in motif II of *Escherichia coli* DNA helicase II render the enzyme nonfunctional in both mismatch repair and excision repair with differential effects on the unwinding reaction. J. Bacteriol. **177:**5612–5621.
9. **Brosh, R. M., Jr., and S. W. Matson.** 1996. A partially functional DNA helicase II mutant defective in forming stable binary complexes with ATP and DNA. J. Biol. Chem. **271:**25360–25368.
10. **Brosh, R. M., Jr., and S. W. Matson.** 1997. A point mutation in *Escherichia coli* DNA helicase II renders the enzyme nonfunctional in two DNA repair pathways. J. Biol. Chem. **272:**572–579.
11. **Clark, A. J., and A. D. Margulies.** 1965. Isolation and characterization of recombination-deficient mutants of *Escherichia coli* K12. Proc. Natl. Acad. Sci. USA **53:**451–459.
12. **George, J. W., R. M. Brosh, and S. W. Matson.** 1994. A dominant negative allele of the *Escherichia coli uvrD* gene encoding DNA helicase II. A biochemical and genetic characterization. J. Mol. Biol. **235:**424–435.
13. **Gilchrist, C. A., and D. T. Denhardt.** 1987. *Escherichia coli rep* gene: sequence of the gene, the encoded helicase, and its homology with *uvrD*. Nucleic Acids Res. **15:**465–475.
14. **Gorbalenya, A. E., and E. V. Koonin.** 1990. Superfamily of UvrA-related NTP-binding proteins: implications for rational classification of repair/recombination systems. J. Mol. Biol. **213:**583–591.
15. **Gorbalenya, A. E., E. V. Koonin, A. P. Donchenko, and V. M. Blinov.** 1988. A novel superfamily of nucleoside triphosphate-binding motif containing proteins which are probably involved in duplex unwinding in DNA and RNA replication and recombination. FEBS Lett. **235:**16–24.
16. **Hodgman, T. C.** 1988. A new superfamily of replicative proteins. Nature **333:**22–23.
17. **Kuhn, B., M. Abeld-Monem, H. Krell, and H. Hoffman-Berling.** 1979. Evidence for two mechanisms for DNA unwinding catalyzed by DNA helicases. J. Biol. Chem. **254:**11343–11350.

18. **Kushner, S. R.** 1974. In vivo studies of temperature-sensitive *recB* and *recC* mutants. J. Bacteriol. **120:**1213–1218.
19. **Kushner, S. R., and V. F. Maples.** 1988. Purification and properties of the UvrD helicase, p. 509–527. *In* E. C. Friedberg and P. C. Hanawalt (ed.), DNA repair: a laboratory manual, vol. 3. Marcel Dekker, Inc., New York, N.Y.
20. **Lohman, T. M., and K. P. Bjornson.** 1996. Mechanisms of helicase-catalyzed DNA unwinding. Annu. Rev. Biochem. **65:**169–214.
21. **Luria, S. E., and M. Delbruck.** 1943. Mutations of bacteria from virus sensitivity to virus resistance. Genetics **28:**491–511.
22. **Maples, V. F., and S. R. Kushner.** 1982. DNA repair in *Escherichia coli*: identification of the *uvrD* gene product. Proc. Natl. Acad. Sci. USA **79:**5616–5620.
23. **Matson, S. W.** 1986. *Escherichia coli* DNA helicase II (*uvrD* gene product) translocates unidirectionally in a 3′ to 5′ direction. J. Biol. Chem. **262:**10169–10175.
24. **Matson, S. W., D. W. Bean, and J. W. George.** 1994. DNA helicases: enzymes with essential roles in all aspects of DNA metabolism. Bioessays **16:**13–22.
25. **Matson, S. W., and K. A. Kaiser-Rogers.** 1990. DNA helicases. Annu. Rev. Biochem. **59:**289–329.
26. **Matson, S. W., and C. C. Richardson.** 1985. Nucleotide-dependent binding of the gene 4 protein of bacteriophage T7 to single-stranded DNA. J. Biol. Chem. **260:**2281–2287.
27. **Mendonca, V. M., K. Kaiser-Rogers, and S. W. Matson.** 1993. Double helicase II (*uvrD*)-helicase IV (*helD*) deletion mutants are defective in the recombination pathways of *Escherichia coli*. J. Bacteriol. **175:**4641–4651.
28. **Miller, J. F.** 1988. Bacterial electroporation. Bio-Rad Lab. Rep. 5.
29. **Modrich, P.** 1991. Mechanisms and biological effects of mismatch repair. Annu. Rev. Genet. **25:**229–253.
30. **Morel, P., J. A. Hejna, S. D. Ehrlich, and E. Cassuto.** 1993. Antipairing and strand transferase activities of *E. coli* helicase II (UvrD). Nucleic Acids Res. **21:**3205–3209.
31. **Orren, D. K., C. P. Selby, J. E. Hearst, and A. Sancar.** 1992. Postincision steps of nucleotide excision repair in *Escherichia coli*. Disassembly of the UvrBD-DNA complex by helicase II and DNA polymerase I. J. Biol. Chem. **267:**780–788.
32. **Peluso, R. W., and G. H. Rosenberg.** 1987. Quantitative electrotransfer of proteins from sodium dodecyl sulfate-polyacrylamide gels onto positively charged nylon membranes. Anal. Biochem. **162:**389–398.
33. **Radman, M.** 1988. Mismatch repair and genetic recombination, p. 169–192. *In* R. Kucherlapati and G. R. Smith (ed.), Genetic recombination. American Society for Microbiology, Washington, D.C.
34. **Rayssingyier, C., D. S. Thaler, and M. Radman.** 1989. The barrier to recombination between *Escherichia coli* and *Salmonella typhimurium* is disrupted in mismatch-repair mutants. Nature **342:**396–401.
35. **Richet, E., and M. Kohiyama.** 1976. Purification and characterization of a DNA-dependent ATPase from *Escherichia coli*. J. Biol. Chem. **251:**808–812.
36. **Richet, E., Y. Nishimura, Y. Hirota, and M. Kohiyama.** 1983. *Escherichia coli uvrD* mutants with thermosensitive DNA-dependent adenosine triphosphatase I (helicase II). Mol. Gen. Genet. **192:**378–385.
37. **Runyon, G. T., D. G. Bear, and T. M. Lohman.** 1990. *Escherichia coli* helicase II (*uvrD*) protein initiates DNA unwinding at nicks and blunt ends. Proc. Natl. Acad. Sci. USA **87:**6383–6387.
38. **Sambrook, J., E. F. Fritsch, and T. Maniatis.** 1989. Molecular cloning: a laboratory manual, 2nd ed. Cold Spring Harbor Laboratory Press, Cold Spring Harbor, N.Y.
39. **Sancar, A.** 1994. Mechanisms of DNA excision repair. Science **266:**1954–1956.
40. **Sibghat-Ullah, A., A. Sancar, and J. E. Hearst.** 1990. The repair patch of *E. coli* (A)BC exinuclease. Nucleic Acids Res. **18:**5051–5053.
41. **Siegel, E. C.** 1981. Complementation studies with the repair-deficient *uvrD3*, *uvrE156* and *recL152* mutations in *Escherichia coli*. Mol. Gen. Genet. **184:**526–530.
42. **Siegel, E. C.** 1973. Ultraviolet-sensitive mutator strain of *Escherichia coli* K-12. J. Bacteriol. **113:**145–160.
43. **Siegel, E. C., and H. Race.** 1981. Phenotypes of UV-sensitive *uvrD3*, *recL152*, and *uvrD156* mutants of *Escherichia coli*. Mutat. Res. **83:**49–59.
44. **Tabor, S., and C. C. Richardson.** 1985. A bacteriophage T7 polymerase/promoter system for controlled exclusive expression of specific genes. Proc. Natl. Acad. Sci. USA **82:**1074–1078.
45. **Van Houten, B., H. Gamper, J. E. Hearst, and A. Sancar.** 1988. Analysis of sequential steps of nucleotide excision repair in *Escherichia coli* using synthetic substrates containing single psoralen adducts. J. Biol. Chem. **263:**16553–16560.
46. **Walker, J. M., M. Sarsate, M. J. Runswick, and N. J. Gay.** 1982. Distantly related sequences in the A- and B-subunits of ATP synthase, myocin, kinases, and other ATP-requiring enzymes and a common nucleotide binding fold. EMBO J. **1:**945–951.
47. **Wang, R.-F., and S. R. Kushner.** 1991. Construction of versatile low-copy-number vectors for cloning, sequencing and gene expression in *Escherichia coli*. Gene **100:**195–199.
48. **Washburn, B. K., and S. R. Kushner.** 1993. Characterization of DNA helicase II from a *uvrD252* mutant of *Escherichia coli*. J. Bacteriol. **175:**341–350.
49. **Washburn, B. K., and S. R. Kushner.** 1991. Construction and analysis of deletions in the structural gene (*uvrD*) for DNA helicase II of *Escherichia coli*. J. Bacteriol. **173:**2569–2575.
50. **Willetts, N. S., and A. J. Clark.** 1969. Characteristics of some multiply recombination-deficient strains of *Escherichia coli*. J. Bacteriol. **100:**231–239.
51. **Zhang, G., L. R. Baugh, E. Deng, C. M. Hamilton, V. F. Maples, and S. R. Kushner.** 1997. Conserved motifs II to VI of DNA helicase II from *Escherichia coli* are all required for biological activity. J. Bacteriol. **179:**7544–7550.
52. **Zieg, J., and S. R. Kushner.** 1977. Analysis of genetic recombination between two partially deleted lactose operons of *Escherichia coli* K-12. J. Bacteriol. **131:**123–132.
53. **Zieg, J., V. F. Maples, and S. R. Kushner.** 1978. Recombination levels of *Escherichia coli* K-12 mutants deficient in various replication, recombination, or repair genes. J. Bacteriol. **134:**958–966.